Supporting information
for

Enhanced XUV harmonics generation with an intense laser field in the overdriven regime

Zhiyong Qin, Zibo Xu, Changhai Yu*, Jiansheng Liu*, Jintan Cai, Zhijun Zhang, Shiyi Zhou, Xuhui Jiao, and Zhongtao Xiang

Department of Physics, Shanghai Normal University, Shanghai 200234, China
* Correspondence: yuchanghai@shnu.edu.cn (C. Y.); liujs@shnu.edu.cn (J. L.)

1. Comparison of single-atom HHG calculated by SFA and TDSE

In order to verify the accuracy of our model, we also carried out the numerical solution of the time-dependent Schrödinger equation (TDSE) of a single helium atom based on a single active electron, and the results are shown in Figure S1 and Figure S2. Figure S1 showed the ionization probability with time at different driving laser intensities calculated by SFA and 3D-TDSE[1], respectively. In the ionization probability calculation, we considered six excited states: 1s2s, 1s2p, 1s3s, 1s3p, 1s4s, and 1s4p. The population of each state with time can be expressed as $P_n(t) = |\langle \phi_n(r)|\varphi(r,t)\rangle|^2$, and the ionization probability with time can be expressed as $p(t) = 1 - \sum_{i=1}^{N} P_i(t)$, where $\phi_n(r)$ is the eigen wavefunction of each state and $\varphi(r,t)$ is the wavefunction at time t. It is worth noting that, though the laser intensity legend labels in the following figures showed 7.5 I_0, 12 I_0, 15 I_0, and 20 I_0, the actual intensities used in the following calculations are approximately 6.8 I_0, 10.2 I_0, 12.2 I_0, and 16.3 I_0, respectively, which is because the intensity legend labels represent the peak laser intensity in a vacuum, but the actual peak intensity is lower due to the propagation effects in the medium, as shown in Figure 3 of the manuscript. It can be seen that the ionization probability obtained by TDSE at different laser intensities is all in good agreement with that obtained by SFA.
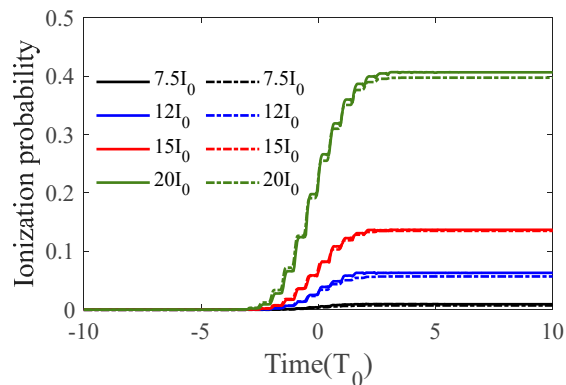

Figure S1 Ionization probability calculated by TDSE (solid line) and SFA model (dashed line). $I_0 = 1 \times 10^{14}$ W/cm^2.

Figure S2 showed the harmonic spectrum calculated by TDSE (red and blue lines) and SFA (black line) at different laser intensities. In the TDSE calculation, we considered two cases of the initial wavefunction, one is a pure ground state ($\varphi_0 = \phi_g$) (red line), and the other is a superposition initial state of the ground and the 6 excited states above ($\varphi_0 = \phi_{sp} = \sum_{i=1}^{N} c_i \phi_i$) (blue line), where c_i is the initial populated coefficient of each state. One

can see that, as the driving laser intensity increases, not only the cutoff harmonics are extended, but also the plateau harmonic intensity is enhanced, and this is consistent for both the SFA and TDSE. In addition, it can also be seen that the single-atom harmonic spectra of TDSE corresponding to the two initial wavefunction cases are generally consistent at each laser intensity, except for significant deviations near the threshold harmonics (shadow region in each panel). In the threshold harmonics region, there is a significant enhancement around H13 for the case of the initial superposition state compared with the initial pure ground state, this can be attributed to the resonance enhancement of the harmonics caused by XUV-free induction decay (xFID) of the excited states[2]. Moreover, it should be noted that even though the initial wavefunction is a pure ground state, the influence of the excited states is also naturally included in the TDSE calculation. It is the periodic oscillations of the excited states' population in the domain center of the driving laser that led to the influence of the excited state becoming less obvious. However, when the initial wave function is a superposition of the ground state and the excited states, the population of the excited states are relatively stable and their influence on the harmonics will be more noticeable. Therefore, there are some studies that use pre-excited states [3,4] or Rydberg states to enhance the HHG intensity [5,6]. Therefore, one can conclude that the effects of the excited states just exist below and near the threshold harmonics, which does not influence the harmonics in the high plateau region and near the cutoff region.

Furthermore, by comparing the HHG spectra of TDSE and SFA, one can see that the cutoff energy of TDSE and SFA is nearly consistent at relatively low laser intensity ($I < 12$ I_0), but there are slight deviations at high laser intensity ($15 I_0$ and $20 I_0$). In the high laser intensity, the cutoff region of TDSE appears flatter compared to SFA, which means that the cutoff energy of TDSE is lower than that of SFA. In addition, the HHG spectra orders of SFA appear clearer compared to the TDSE, which may be attributed to the fact that the HHG of the SFA only takes the transition of the ground state and the continuum state into consideration, but the HHG of the TDSE includes the contributions from all the excited states.
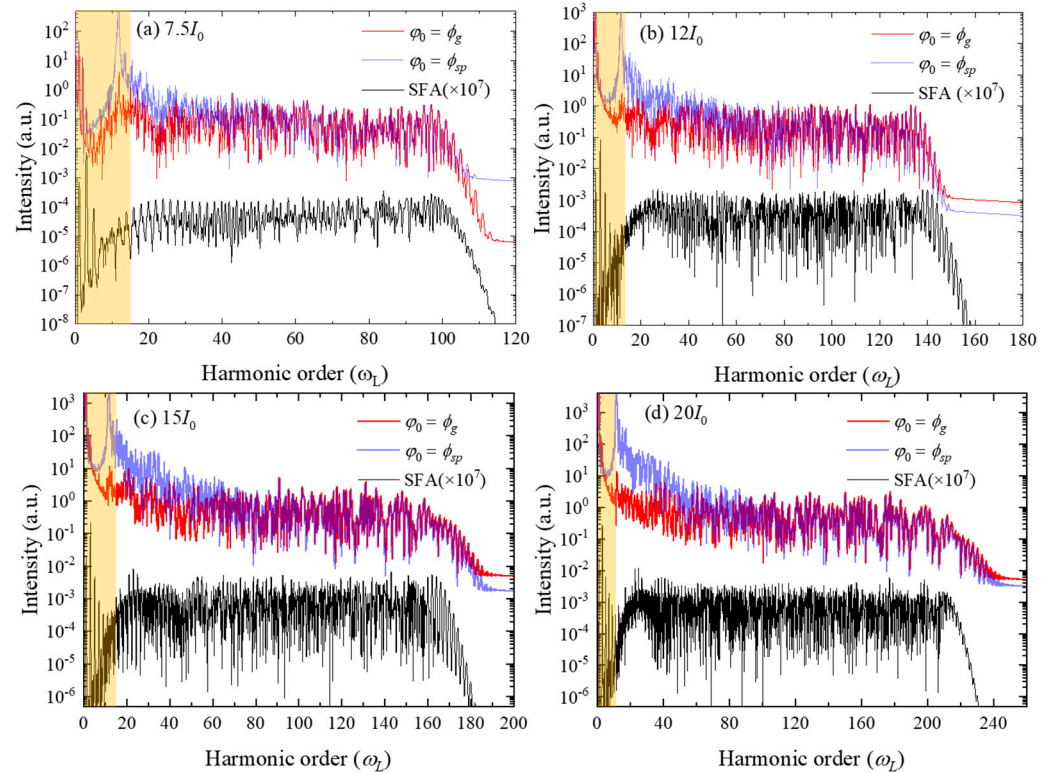

Figure S2. HHG spectrum of single-atom response calculated by TDSE and SFA (black line) at different laser intensities. In the TDSE calculation, two initial state cases are considered: the initial pure ground state (red line) and the initial superposition state of

the ground and six excited states (blue line). The shadow region represents the harmonics below the threshold.

In order to clearly investigate the influence of the laser intensity on the harmonic intensity in the microscopic, we also calculated the average intensity of harmonic order from H65 to H95 in Figure S2 at each laser intensity, as shown in Figure S3, in which the harmonic intensity has been normalized. It can be seen that the evolution trend of the harmonic intensity calculated by both the SFA and TDSE is in agreement with each other; namely, the harmonic intensity increase with the laser intensity until saturation, which is consistent with the results of previous studies [7,8]. This is because the HHG is dependent on tunnel ionization, but excessive ionization would lead to the depletion of the ground state, which will prevent harmonic enhancement. In our simulations, the saturation intensity is higher than 20 I_0. As the intensity exceeds saturation, the growth of harmonics will decelerate, and the cutoff order will deviate from the expected cutoff formula. Nevertheless, within the range of laser intensity we are considering, the results of SFA and TDSE are in good agreement with each other in the plateau and near the cutoff region.
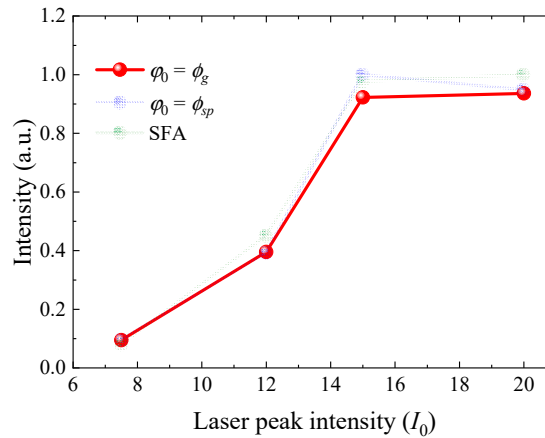

Figure S3. The normalized average intensity of harmonics from H65 to H95 with different laser intensities was calculated by TDSE and SFA.

In conclusion, we have compared the HHG of the single-atom response calculated by the SFA and TDSE. Although the TDSE includes the effects of the excited states, the ionization probability of SFA and TDSE at each laser intensity is nearly the same as each other. Furthermore, by comparing the HHG spectra of SFA and TDSE, we find that the excited states only affect harmonics near the threshold and do not influence the harmonics of interest in the high plateau region, and the average intensity from H65 to H95 calculated by the SFA and TDSE with laser intensity shows the same trend, that is, the intensity increases with the increase in laser intensity until saturation. It should be noted that all the findings above are preliminary and just limited to the currently considered laser intensity range, that is, the laser intensity ≤20 I_0. For a higher laser intensity, the effect of the excited state on the harmonic spectrum and intensity may be different and more pronounced, which should be more accurately simulated based on TDSE. Nevertheless, we believe that in our current work, SFA is accurate enough to describe our findings in the manuscript.

References for supporting information

1.   Fu, Y.; Zeng, J.; Yuan, J. PCTDSE: A parallel Cartesian-grid-based TDSE solver for modeling laser–atom interactions. *Comput. Phys. Commun.* **2017**, *210*, 181-192, doi:https://doi.org/10.1016/j.cpc.2016.09.016.

2.   Beaulieu, S.; Camp, S.; Descamps, D.; Comby, A.; Wanie, V.; Petit, S.; Légaré, F.; Schafer, K.J.; Gaarde, M.B.; Catoire, F.; et al. Role of Excited States In High-order Harmonic Generation. *Phys. Rev. Lett.* **2016**, *117*, 203001, doi:10.1103/PhysRevLett.117.203001.

3.   Watson, J.B.; Sanpera, A.; Chen, X.; Burnett, K. Harmonic generation from a coherent superposition of states. *Phys. Rev. A* **1996**, *53*, R1962-R1965, doi:10.1103/PhysRevA.53.R1962.

4.   Yuan, X.; Wei, P.; Liu, C.; Zeng, Z.; Zheng, Y.; Jiang, J.; Ge, X.; Li, R. Enhanced high-order harmonic generation from excited argon. *Appl. Phys. Lett.* **2015**, *107*, 041110, doi:10.1063/1.4927662.

5.   Chen, J.; Wang, R.; Zhai, Z.; Chen, J.; Fu, P.; Wang, B.; Liu, W.-M. Frequency-selected enhancement of high-order-harmonic generation by interference of degenerate Rydberg states in a few-cycle laser pulse. *Phys. Rev. A* **2012**, *86*, 033417, doi:10.1103/PhysRevA.86.033417.

6.   Tikman, Y.; Yavuz, I.; Ciappina, M.F.; Chacón, A.; Altun, Z.; Lewenstein, M. High-order-harmonic generation from Rydberg atoms driven by plasmon-enhanced laser fields. *Phys. Rev. A* **2016**, *93*, 023410, doi:10.1103/PhysRevA.93.023410.

7.   Krause, J.L.; Schafer, K.J.; Kulander, K.C. High-order harmonic generation from atoms and ions in the high intensity regime. *Phys. Rev. Lett.* **1992**, *68*, 3535-3538, doi:10.1103/PhysRevLett.68.3535.

8.   Miyazaki, K.; Takada, H. High-order harmonic generation in the tunneling regime. *Phys. Rev. A* **1995**, *52*, 3007-3021, doi:10.1103/PhysRevA.52.3007.